scientific reports

OPEN

A comprehensive single-cell RNA transcriptomic analysis identifies a unique SPP1+ macrophages subgroup in aging skeletal muscle

Wen Bi[1], Mengyue Yang[4], Mengjia Shi[5], Mirong Hou[6], Changqing Jiang[1], Gang Fan[3✉] & Weiming Guo[1,2✉]

Senescence of skeletal muscle (SkM) has been a primary contributor to senior weakness and disability in recent years. The gradually declining SkM function associated with senescence has recently been connected to an imbalance between damage and repair. Macrophages (Mac) are involved in SkM aging, and different macrophage subgroups hold different biological functions. Through comprehensive single-cell transcriptomic analysis, we first compared the metabolic pathways and biological functions of different types of cells in young (Y) and old (O) mice SkM. Strikingly, the Mac population in mice SkM was also explored, and we identified a unique Mac subgroup in O SkM characterized by highly expressed SPP1 with strong senescence and adipogenesis features. Further work was carried out on the metabolic and biological processes for these Mac subgroups. Besides, we verified that the proportion of the SPP1+ Mac was increased significantly in the quadriceps tissues of O mice, and the senotherapeutic drug combination dasatinib + quercetin (D + Q) could dramatically reduce its proportion. Our study provides novel insight into the potential role of SPP1+ Mac in SkM, which may serve as a senotherapeutic target in SkM aging.

Keywords Single-cell sequencing, Skeletal muscle, SPP1+ macrophages, Cell senescence, Senolytics

The rise in the worldwide population's age demographic promotes a concentration on senescence-related diseases and scientific investigations. Neurological disorders associated with aging, such as mental disorders and cognition impairment, as well as cardiovascular diseases like coronary heart disease, seem to gain more focus than skeletal muscle aging[1]. However, research has suggested that the elderly (> 60-year-old) have a gradual decrease in muscle mass, approximately at a speed of 1–2% per year, which results in disturbances in nerve and muscle coordination, thus increasing the fall risk[2,3]. Skeletal muscle (SkM) aging is characterized as a degenerative age-related reduction in mass and function, fat infiltration, angiogenesis, and other tissue modifications, which is a major cause of life quality decline in the elderly[4].

Macrophages (Mac) are the main type of immune cells found in SkM, and they are primarily distributed in the perimysium and endomysium regions[5]. The infiltration of macrophages in SkM plays a crucial role in the processes of damage healing and regeneration[6]. In detail, Mac could adopt various polarizations to serve specific roles throughout distinct phases of the healing process after injury[7]. Immunometabolism of Mac has been expounded to play a vital role in SkM regeneration. Detailedly, they can chew up debris, generate plentiful cytokines and growth factors, and enroll other immune cells. Meanwhile, macrophages are also involved in metabolic remodeling and inflammation, that is, lactate-polarized Mac exert an anti-inflammatory function and facilitate SkM angiogenesis and regeneration[8,9]. Previous literatures reported a decreased inflammatory response that macrophage involved during aged human SkM regeneration[10,11]. Specifically, as an anti-inflammatory subtype in

[1]Department of Sports Medicine, The Sixth Affiliated Hospital of Shenzhen University, Shenzhen Nanshan People's Hospital, Shenzhen 518052, China. [2]Department of Orthopaedics, Affiliated Hospital of Guilin Medical College, Guilin 518052, China. [3]Department of Urology, The Sixth Affiliated Hospital of Shenzhen University, Shenzhen Nanshan People's Hospital, Shenzhen 518052, China. [4]Department of Cardiology, The Sixth Affiliated Hospital of Shenzhen University, Shenzhen Nanshan People's Hospital, Shenzhen 518052, China. [5]Department of Traditional Chinese Medicine, The First Affiliated Hospital of Guangzhou Medical University, Guangzhou 510120, China. [6]Cancer Institute of Traditional Chinese Medicine, Longhua Hospital, Shanghai University of Traditional Chinese Medicine, Shanghai 200030, China. ✉email: gang.fan.med@qq.com; 253779211@qq.com

Mac, elevated M2a macrophages is seen in aging SkM and contribute to SkM fibrosis[12]. Krasniewki et al.[13] have demonstrated Mac classification and the alteration of Mac in the process of SkM aging. However, the function of senescence-associated Mac in SkM and the efficacy of senolytics on this Mac subpopulation remain to be resolved.

To fill this gap, we investigated and compared the distinct cell types and the metabolism of Mac in SkM between Y and O from publicly accessed single-cell datasets using the comprehensive bioinformatics method. An exclusive subgroup of macrophages with markedly elevated SPP1 expression was discovered in aging SkM, and such a group of Mac demonstrates an increased adipogenesis feature and more senescent cell characteristics. Importantly, we verified that the proportion of SPP1+ Mac was increased significantly in O mice and diminished in the D + Q group in vivo. Our findings indicated that drug intervention targeting cellular senescence in SkM could relieve Mac senescence, which provides a potential senotherapeutic target for countering SkM aging.

Method

Data acquisition and processing

The single-cell mRNA sequence (scRNA-seq) datasets used consist of GSE143437, GSE172410, GSE162172, GSE232106, and GSE195507, available for free download via the GEO database. GSE143437 contained 3 samples of mouse SkM tissues from young mice aged 4–7 months; GSE172410 comprised 3 Y (6 months) and 3 old (24 months) SkM samples. GSE162172 involved 4 old (20-month-old) mice SkM samples. GSE232106 included 4 old (26 months) mice SKM samples. As for GSE195507, it contained 9,469 mouse SkM macrophages from 3 young (3 months) and 3 old (22–24 months) mice (Supplementary Table 1).

The downloaded raw data were processed with the Seurat package (version 5.0.1;) and integrated with the "Harmony" algorithm in R software (version 4.3.0) for each sample[14,15]. Regarding the integrated data and the macrophage data, cell profiles were filtered employing the criteria of the original publications[13,16–19]. The data were then normalized using the "LogNormalize" method, and marker genes for each cluster were recognized using the "FindMarkers" function[20]. Identification of cell types using the marker genes of each cluster and then mapping to the Panglao website (https://panglaodb.se/index.html)[21]. The UMAP method was utilized to visualize the identified cell clusters. The "Addmodulescore" function was adopted to compute the scores of biological processes in distinct groups.

Functional enrichment analysis

Enrichment analysis between young and old skeletal muscle cell types in mice was conducted via Metascape (https://metascape.org/), with $p < 0.01$ as selection criteria and then top 10 items were visualized using the ggplot2 package in R[22]. We conducted 4 approaches for enrichment analysis across different clusters: ssGSEA, AUCell, UCell, and singscore. "irGSEA" was adopted to visualize the results.

"SenMayo" gene set

The gene collection "SenMayo" was employed to access cellular senescence, which has been verified across species in both scRNA-seq and bulk RNA sequencing[23]. It had higher validation efficiency than common gene sets linked to senescence[24].

Metabolism pathway analysis

For the analysis and inference of the metabolic activities of distinct cell types and macrophages in both young and old mice SkM, following the conversion of mouse gene symbols to their human one-to-one orthologs using the "convert_mouse_to_human_symbols" function in the "nichenetr" algorithm[25], the "scMetabolism" package was utilized to calculate the metabolic activities at the single-cell level[26].

Pseudotime trajectory analysis

Trajectory analysis of SkM macrophages was implemented by the "learn graph" function in the Monocle 3 algorithm (https://cole-trapnell-lab.github.io/monocle3/)[27,28]. Information about grouping and clustering was derived from "UMAP" in Seurat. To filter out the co-regulated genes as SPP1, the function "find genes modules" was employed.

Cell–cell communication analysis

Inference and analysis of the intercellular communication network at the single-cell level were conducted via the CellChat algorithm (version 1.1.0). SkM macrophages from young and old mice were separately analyzed and exhibited[29].

Protein–protein interaction (PPI) network

Following the PPI network's construction using the genes in the same modules as SPP1, analysis, and visualization were conducted by the STRING website (https://cn.string-db.org/)[30]. Meanwhile, these genes were subjected to enrichment analysis via four selected databases: KEGG, GO, Wikipathway, and Reactome.

Cell cycle analysis

For predicting the cell cycle distributions of the SPP1+ macrophage subpopulation, the CellCycleScoring function in the Seurat package was conducted. This function used previously defined S/G2M marker genes to confirm the phases[31].

Samples were taken of SkM from young and old mice

C57BL/6 male mice were purchased from Dossy Experimental Animals Co., LTD (Chengdu, China). Animal study protocols were strictly authorized by the animal care committee of Shenzhen Nanshan People's Hospital, we confirmed all methods were conducted in accordance with the relevant guidelines and regulations and ensured there were no ethical concerns. All mice were thoroughly anesthetized using isoflurane followed by cervical dislocation, and then the body composition (total body lean and fat mass) of young and old mice was obtained by quantitative MRI (EchoMRI-100; Houston, TX, USA) as illustrated previously[32]. Finally, the quadriceps muscle tissues were removed. Young (4 months old) and old (22 months old) mice were maintained at the animal feeding center of Shenzhen Nanshan People's Hospital.

Senolytics treatment
18-month-old mice were gavaged with a senolytics cocktail, including dasatinib (5 mg/kg) (D) plus quercetin (50 mg/kg) (Q), as previously described[16,33]. In brief, D + Q was dissolved by 10% polyethylene glycol400 (PEG 400; Sigma-Aldrich, #2532268). Finally, mice were administered with D + Q or vehicle (10% PEG 400) for three continuous days biweekly for 4 months.

Immunofluorescence staining and macrophage quantification
Quadriceps muscles from 3 young and 3 old mice were harvested and washed with phosphate buffer saline (PBS, Thermo Fisher, USA). Then, samples were subjected to rapid freezing using liquid nitrogen and stored at − 80 °C until use. Samples were embedded using an optimal cutting temperature compound (OCT, Sakura, USA) at − 22 °C. After that, the quadriceps tissues were cut to a thickness of 15 μm. Primary antibodies against F4/80-rabbit (Boster, A08751, 1: 100 dilution), the canonical marker of macrophages in mice. Anti-SPP1-mouse (Santa Cruz, sc-21742, 4 μg/ml), the special genetic marker of SPP1+ macrophages. Anti-Laminin-rabbit (Boster, BA1761-1, 1:100). The secondary antibodies against three markers were Alexa Fluor 647-labeled goat anti-rabbit antibody (Abcam, ab150083, 1:400) for F4/80 and Laminin; Alexa Fluor 488-labeled goat anti-mouse antibody (Beyotime, A0428, 1:400) for SPP1, respectively. An anti-fluorescence quenched sealing solution (Beyotime, P0131, DAPI included) was added to each sample before visualizing the slides using laser confocal microscopy (FV3000, Olympus). Finally, five photographs were taken using the 20 × lens, and the images were processed and analyzed by ImageJ for macrophage quantification.

Statistical analysis
The software R (v. 4.3.0) and GraphPad Prism (v.9.5.1) completed the statistical work. Comparisons between the two groups were conducted with the student's unpaired t-test or Wilcoxon test. The correlation analysis of the two groups was carried out via Spearman correlation analysis. p value under the threshold of 0.05 was considered statistically significant.

Ethics approval

Experiments involving mice in this study were authorized and approved by the Animal Care Committee of Shenzhen Nanshan People's Hospital.

Results

Data merge and quality control

Information for single-cell transcriptomes, including mouse SkM and SkM macrophages, was exhibited in Supplementary Table 1. Samples in each dataset were filtered based on original studies[16–19], then merged using the "merge" function in the Seurat package, and the batch effect was removed using the "Harmony" method. Finally, 34,067 cells were obtained and further classified into 16 clusters (Fig. 1A,B).

Single-cell profiling of SkM from young and old mice

Canonical cell type markers (Supplementary Table 2) were implemented to identify different SkM cell types (Figs. 1C, S1, and S2)[34]. The 16 cell clusters were then divided into 11 cell types, which were labeled as endothelial cells (ECs), fibroadipogenic progenitors (FAPs), myonuclei, pericytes, smooth muscle cells, macrophages, neurons, tenocytes, satellite cells, neutrophils, B cells. A small group of cells was hard to identify and labeled as unknown (Fig. 1D). Furthermore, we calculated the proportion of these cell subpopulations between Y and O mice. ECs and FAPs were the most prevalent cell types, and satellite cell abundance was lower in O SkM, as previously reported[16] (Fig. 1E).

Lyve1⁻/MHCII⁺ is the main type of macrophage in the mouse SkM

As macrophages played a vital role in SkM regeneration and aging[9,13], we took the macrophage cells group to sub-cluster analysis. Macrophages were divided into six clusters when the resolution was set as 0.3. We identified four cell groups from the six clusters (Fig. 2A). They were: (0) 294 macrophages highly expressed *C1qa, C1qb, C1qc, H2-Aa* and *H2-Eb1*; (1) 230 macrophages highly expressed *Lyve1, Folr2* and *Mrc1*; (2) 213 macrophages highly expressed *Gngt2, Hp* and *Gsr*; (3) 200 macrophages highly expressed *H2-Aa*, *H2-Eb1, H2-DMb1, Lyz1* and *Fn1* (Fig. 2B–D). They were further classified into 4 cell groups based on the surface markers Lyve1 and MHC-II and 4 groups based on marker genes (Fig. 2E–F). We found that Lyve1−/MHCII+ was the largest group of macrophages, accounting for approximately 40% of the total macrophages (Fig. 2G). Another large single-cell database of SkM macrophages was used for further verification and investigation. After screening and quality control, 9,469 cells were classified into 11 clusters based on previous studies[13]. Marker genes for each cell cluster
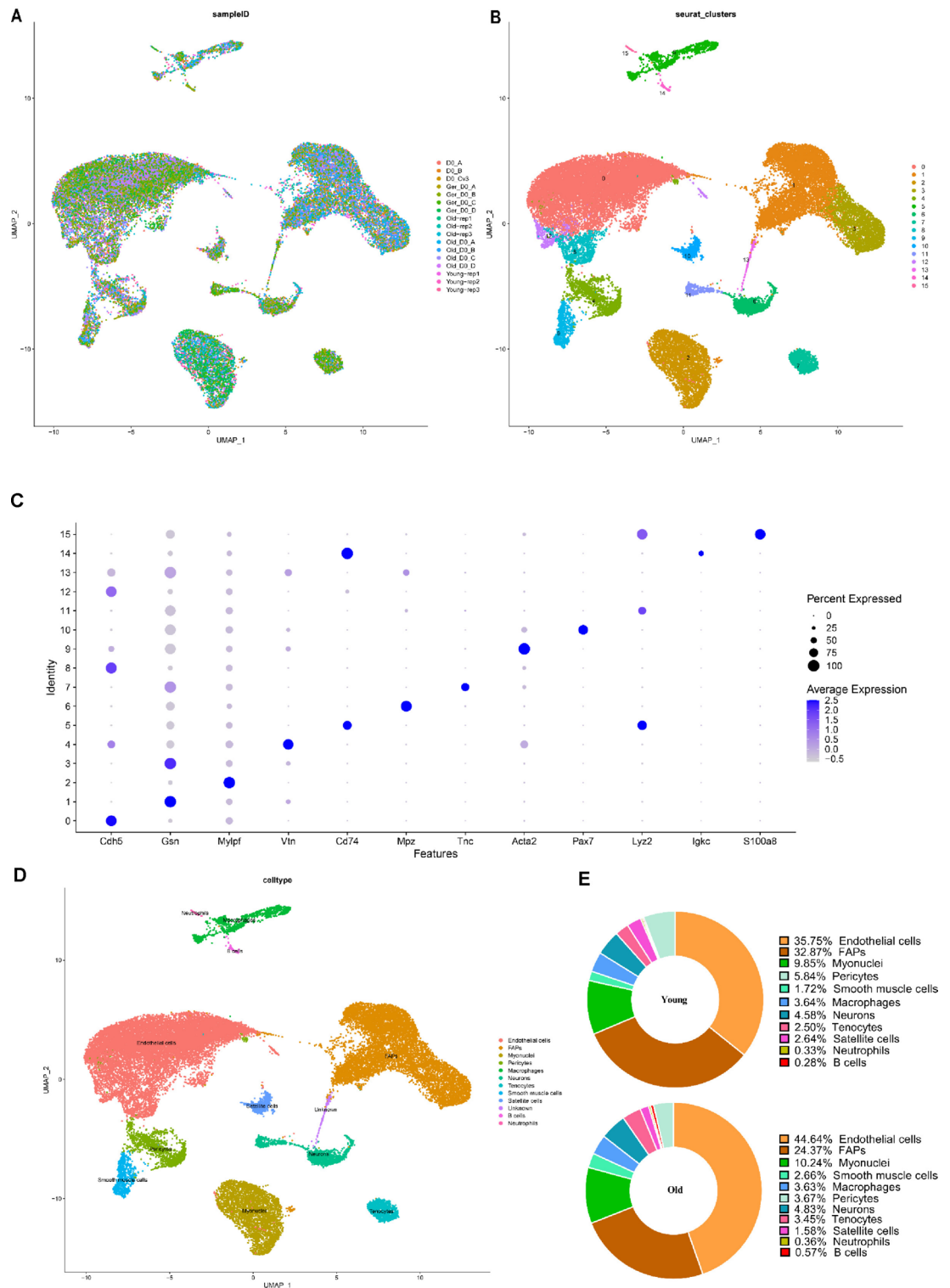
Figure 1. Integration with Harmony method. (**A**) Skeletal muscle samples from 6 young, 7 old, and 4 geriatric mice were integrated with the Harmony method. (**B**) 16 clusters were recognized by Seurat 5.0.1. (**C**) Bubble plot showing the canonical markers of each cell type. (**D**) UMAP plot depicting the cell type in skeletal muscle. (**E**) Relative abundance of distinct cell types at different age in mice SkM.

were exhibited in Supplementary Table 3. Finally, 11 types of SkM macrophages were identified; they were: (0) 2897 cells of highly expressed *Lyve1, Folr2,* and *Mrc1*, which is similar to cluster 1 of the former dataset; (1) 1565 cells of highly expressed *Lyve1* and *Cd209a*; (2) 1494 cells highly expressed *Lyz1* and *Fn1*, which corresponding
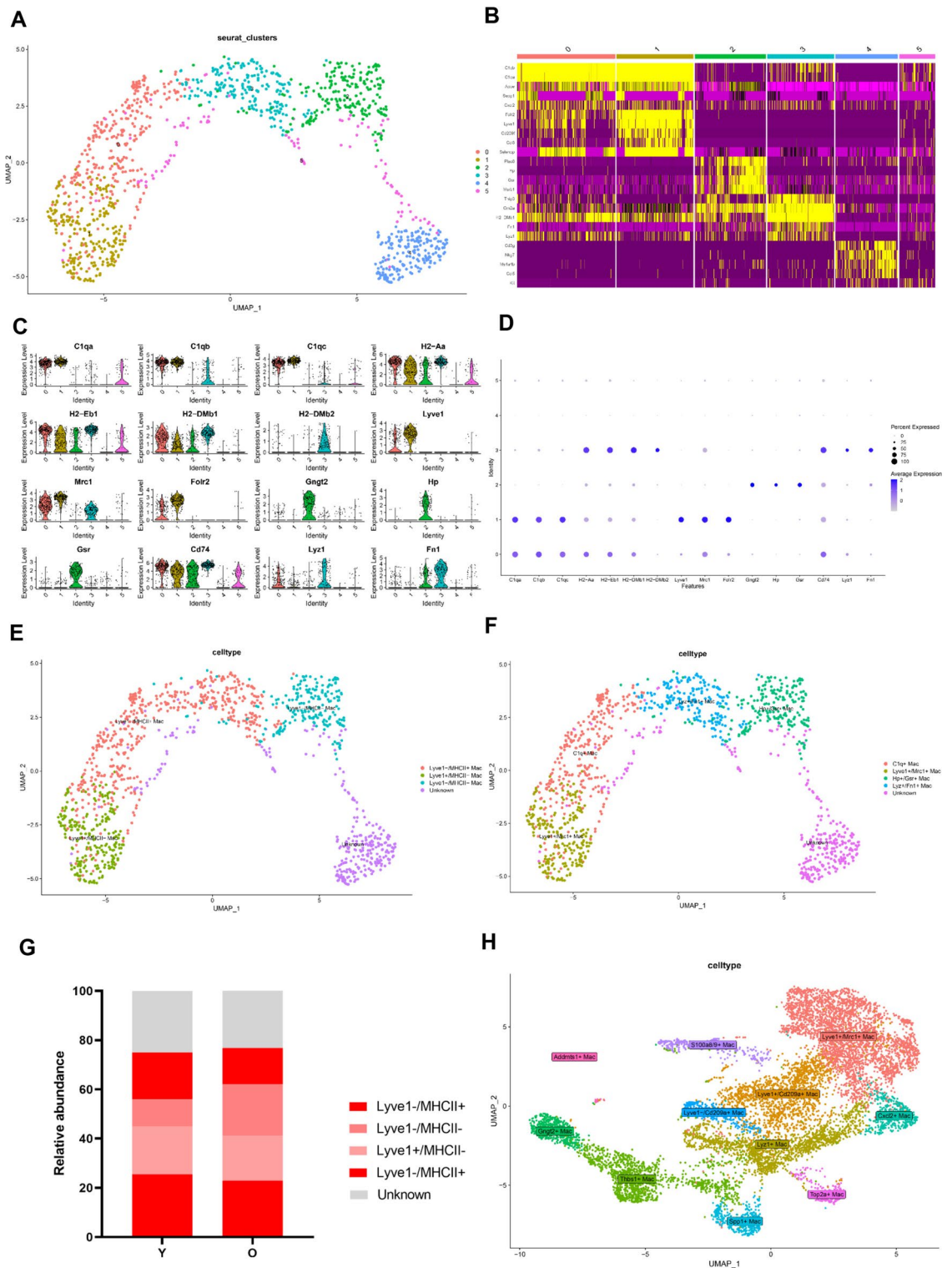
Figure 2. Subclusters of macrophages and marker genes of each cluster in mice SkM. (**A**) The UMAP plot of the six identified clusters. (**B**) The heatmap, violin plot (**C**) and the dot plot (**D**) showing the representative markers across six clusters. (**E**) The UMAP plot illustrating the macrophages subgroups based on the Lyve1/MHCII expression levels and (**F**) their marker genes. (**G**) The relative abundance of macrophages subgroups in young and old mice SkM based on Lyve1/MHCII classification. (**H**) The UMAP plot representing 11 distinct SkM macrophages subgroups based on marker genes in GSE195507.

to cluster 3 of the former dataset; (3) 1320 cells highly expressed *Thbs1*, *Hp*, and *Gsr*, which was homologous to cluster 2 of our dataset; (4) 498 cells highly expressed *Gngt2*; (5) 430 cells highly expressed *Cxcl2* and *Tnf*. (6) 416 cells highly expressed *Spp1*, *Fabp5* and *Gpnmb*; (7) 294 cells highly expressed Cd209a, *H2-Ab1*, *H2-Eb1*; (8) 283 cells highly expressed *S100a8* and *S100a9*; (9) 226 cells highly expressed *Top2a* and *Mki67*. (10) 46 cells highly expressed *Adamts1* and *Sparcl1* (Fig. S3). Krasniewski et al. discovered that Lyve1−/MHCII+ macrophages comprise 39.97% of all macrophages, and they also elaborated the function and polarization of these 11 macrophage subclusters[13], which further confirmed our conclusion (Fig. 2G). Overall, this large single-cell data of SkM macrophages from Krasniewki et al. identified 11 clusters of different macrophages, of which CI0, CI2, and CI3 correspond to cluster 1, cluster 3, and cluster 2 of our dataset, respectively (Fig. 2H). We also confirmed that Lyve1−/MHCII+ is the main type of macrophage in the mouse SkM. However, its function and role in SkM aging should be further elucidated.

Functional enrichment between young and old skeletal muscle from the same subset of Mac

Differently expressed genes between various Mac subpopulations in young and old SkM were analyzed by selecting the top 200 up-regulated genes and the top 200 down-regulated genes within the same cell group for enrichment analysis using the Metascape platform[22]. SPP1+ Mac, S100a8/9+ Mac, and Gngt2+ Mac were ruled out because they mainly disturbed in old skeletal muscle, and Adamts1+ Mac was excluded because of its small number[13]. Most up-regulated genes in old mice SkM macrophages were enriched in terms related to lipid metabolism, including phospholipid dephosphorylation, membrane lipid metabolic process, Ether lipid metabolism, etc., inflammation including regulation of interleukin − 6 production, positive regulation of chemokine production, etc. Most down-regulated genes in old SkM macrophages are mainly enriched in terms such as mitochondrial biogenesis, immune response-regulating signaling pathway, etc. Meanwhile, some signaling pathways, including Selenium metabolism selenoproteins, were shown in almost all cell clusters; however, several pathways, like positive regulation of cholesterol efflux and white fat cell differentiation, were only found in certain Mac subgroups, which demonstrated the homogeneity and heterogeneity of response to signals in distinct Mac subgroups of SkM (Fig. 3).

A landscape of enrichment analysis between different subpopulations of SkM macrophage

Enrichment analysis was implemented on 11 SkM macrophage subpopulations using AUCell, UCell, singscore, and ssgsea to further demonstrate their homogeneity and heterogeneity. Adipogenesis, which has been proven to be increased in aged SkM[5], was found to be up-regulated in SPP1+ macrophages but down-regulated in Cxcl2+ macrophages, which suggests SPP1+ Mac might be involved in the formation of intermuscular adipogenesis during skeletal muscle aging. Angiogenesis, a biological process associated with aging[35], was discovered to be up-regulated in SPP1+ Mac and Addmts1+ macrophages but down-regulated in Lyve1−/Cd209a+ Mac and Thbs1+ Mac. In addition, the TNFA-SIGNALING-VIA-NFKB pathway, the INTERFERON-ALPHA-RESPONSE pathway, and the INTERFERON-GAMMA-RESPONSE pathway were revealed to be down-regulated in SPP1+ Mac. In Lyve1+/Cd209a+ Mac, the TNFA-SIGNALING-VIA-NFKB pathway and the IL6-JAK-STAT3-SIGNALING pathway were shown to be markedly up-regulated (Fig. 4A). Figure 4B exhibited that the results explored by these four methods were principally compatible. Figure 4C suggested a markedly increased activity of adipogenesis, angiogenesis, oxidative phosphorylation, and protein secretion pathways in SPP1+ Mac. Our study found that in the subpopulations of Mac primarily distributed in aging mice SkM, angiogenesis, adipogenesis, and senescence-associated pathways were up-regulated.

SPP1+ Mac owned more senescent characteristics and stronger adipogenesis ability

Adipogenesis has been verified as a potential factor in SkM aging[5,35]. We, therefore, attempted to calculate the adipogenesis and senescence score of 11 SkM macrophage subpopulations in young and old mice SkM. Macrophages in the skeletal muscle of old mice had a greater adipogenesis score than those in young mice, although there was no significant difference in senescence score. Among all macrophage subgroups, SPP1+ Mac scored the highest. (Figs. 5A,B, S4A,B). Correlation analysis confirmed that adipogenesis had a strong linkage with senescence (R = 0.35, $p < 2.2e{-}16$, Fig. 5C). Cell cycle analysis of the young and old skeletal muscle Mac was then performed, respectively. Compared with Mac in young mice SkM, macrophages in old mice SkM were prone to be in the S phase, macrophages in the G2M phase remained almost unchanged, and the G1 phase was decreased, suggesting that cell cycle arrest might be involved in SkM aging (Fig. 5D). Further study verified that SPP1 was up-regulated remarkedly in SPP1+ Mac of old mice SkM compared with that in SKM of young mice (Fig. 5E), and SPP1 expression was significantly increased in macrophages of old mice SkM and mainly expressed at SPP1+ Mac (Fig. 5F). Eventually, scMetabolism was implemented to speculate the metabolism activity of SkM macrophage subpopulations at single-cell resolution. SPP1+ Mac showed the most active metabolic pathways compared to other macrophage subgroups (Fig. S5). Terms linked to lipid metabolism, including Glycerophospholipid metabolism, Ether lipid metabolism and Sphingolipid metabolism, and carbohydrate metabolism, including Glycolysis/Gluconeogenesis and energy metabolism like Oxidative phosphorylation, were found to be significantly up-regulated in macrophages of old mice SkM (Figs. 5G, S6A). Correlation analysis was then conducted between Glycerophospholipid metabolism score, Senmayo score, and adipogenesis score. Our findings proved that Senmoyo Score significantly correlated with the Glycerophospholipid metabolism positively (R = 0.38, $p < 0.001$, Fig. S6B). Further study uncovered that SPP1+ Mac had an increased activity in lipid metabolism like Glycerolipid metabolism, Sphingolipid metabolism, and Steroid metabolism (Figs. 5H, S7). Our study unveiled that SPP1+ Mac holds significant senescent features and enhanced adipogenesis ability via bioinformatic analysis. Additionally, the differences in metabolic pathways were also explored between SkM macrophages in young and old mice.

Figure 3. The dot plot exhibiting the homogeneity and heterogeneity in SkM macrophages subpopulations in Y and O mice.

Pseudo-time analysis of macrophages from young and old mice SkM

Previous studies have reported the polarization of SkM macrophages under different circumstances, for example, inflammation, muscle regeneration, and aging[5,36]. Pseudo-time analysis with Monocle 3 provides a robust tool to explore the state transition of macrophages during aging, inferring cell polarization based on gene expression patterns. Using this method, the polarization trajectories of young and old macrophages between these subgroups were then further investigated, respectively. Most of the macrophages in young mice SkM went
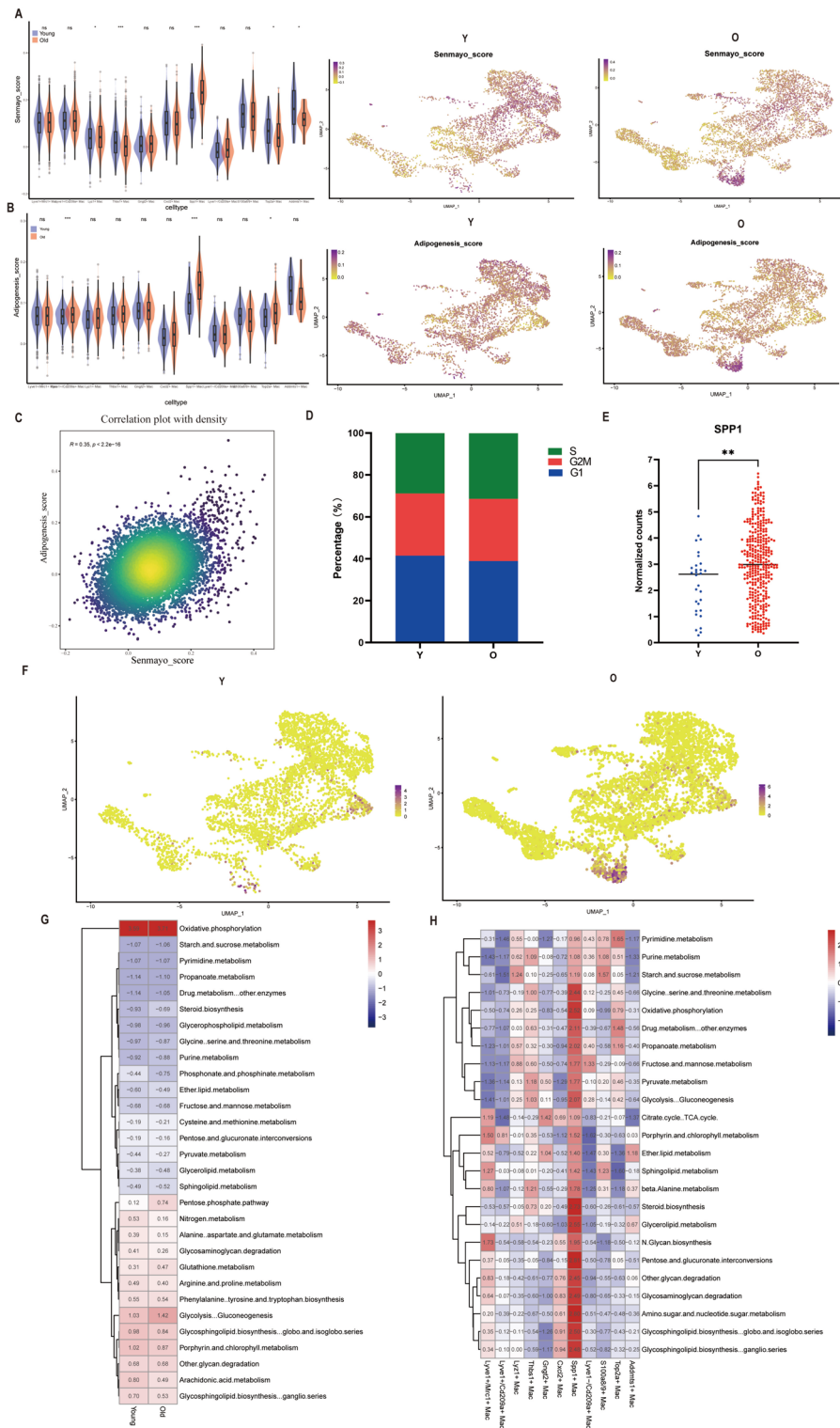
Figure 4. Comprehensive enrichment analysis of different subpopulations of mice SkM macrophages. (**A**) Functional enrichment analysis of gene signature from GSEA. (**B**) The bar plot illustrating the number and proportion of up, down and no significant genes with 4 distinct methods. (**C**) Density scatterplots and density heatmaps exhibiting representative up or down-regulated pathways.

through a polarization trajectory from Lyve1+/Mrc1+ Mac to Lyve1+/Cd209a+ Mac then to Lyz1+ Mac finally to Thbs1+ Mac (Fig. 6A,B, S8A). Top ten genes that had the most significant changes during the trajectory were exhibited in Fig. 6C. To study further, Lyve1+/Mrc1+ Mac, Lyve1+/Cd209a+ Mac, Lyz1+ Mac, and Thbs1+ Mac were extracted to be re-analyzed. The immune response-regulating signaling pathway was shown to be activated along with the pseudo-time trajectory. Additionally, the immune response-regulating signaling pathway-related genes were down-regulated in aging mice SkM macrophages, which was in line with previous enrichment analysis (Fig. 6D,E), proving that the immune response-regulating signaling pathway participated important role in the polarization of SkM macrophages in Y mice. Following that, the relationship between Lyve1+/Mrc1+ Mac, Lyve1+/Cd209a+ Mac, Lyz1+ Mac and Thbs1+ Mac was further analyzed by the pseudo-time method. The results show Lyz1+ Mac served as a state between Lyve1+/Mrc1+ Mac and Thbs1+ Mac (Fig. 6F,G).

In old SkM macrophages, Lyve1+/Mrc1+ Mac distributed at the beginning of the trajectory, Lyz1+ Mac followed, SPP1+ Mac and Thbs1+ Mac were seen throughout the trajectory, and Gngt2+ Mac arrived at the end of the trajectory. These results were in compliance with previous observations from Krasniewski et al. (Figs. 6H, S7B)[13]. Meanwhile, the top 10 genes related to the pseudo-time were identified (Fig. 6J). To explore the complicated association between Lyve1+/Mrc1+ Mac, Lyz1+ Mac, SPP1+ Mac, Thbs1+ Mac, and Gngt2+ Mac, these cells were figured out and re-analyzed. Lyve1+/Mrc1+ Mac was located at the beginning of the trajectory, followed by Lyz1+ Mac, then SPP1+ Mac and Thbs1+ Mac, and Gngt2+ Mac was at the end of the trajectory (Figs. 6I, S8A). Modules of co-regulated genes were then analyzed to illustrate the role of SPP1 better. Finally, 92 modules were identified (Supplementary Table 4). PPI network analysis was then conducted to explore co-regulated genes in highly related modules involving SPP1 (Fig. S8B). The results indicated that SPP1-related genes are involved in osteoclast signaling, antigen processing-cross presentation, ROS and RNS production in phagocytes, metabolic pathways, etc. These results exhibited that SPP1 might participate in amino sugar and nucleotide sugar metabolism and proteasome degradation as well as membrane protein complex (Fig. 6K). Briefly speaking, the polarization trajectories in SkM macrophages of young mice were identified, suggesting that the immune

Figure 5. Characterization of SPP1+ macrophages in mice SkM. (**A**) The violin plot and the UMAP plot showing the distinction in Senmayo score in subgroups of mice young and old SkM macrophages. (**B**) The violin plot and the UMAP plot showing the distinction in adipogenesis score in subgroups of mice Y and O SkM macrophages. (**C**) The correlation plot exhibiting relation between adipogenesis and cellular senescence. (**D**) The bar plot showing the proportion of cell cycle in SkM macrophages of Y and O mice. (**E**) Comparison of SPP1 expression level in SPP1+ macrophages of Y and O mice SkM using scatterplot. (**F**) SPP1 expression level in SkM macrophages in Y and O mice using UMAP plot. (**G**) The heatmap showing metabolic pathway between Y and O macrophages of mice SkM. (**H**) The heatmap showing metabolic pathways in distinct macrophages subgroups of mice SkM. Y, young. O, old. SkM, skeletal muscle.
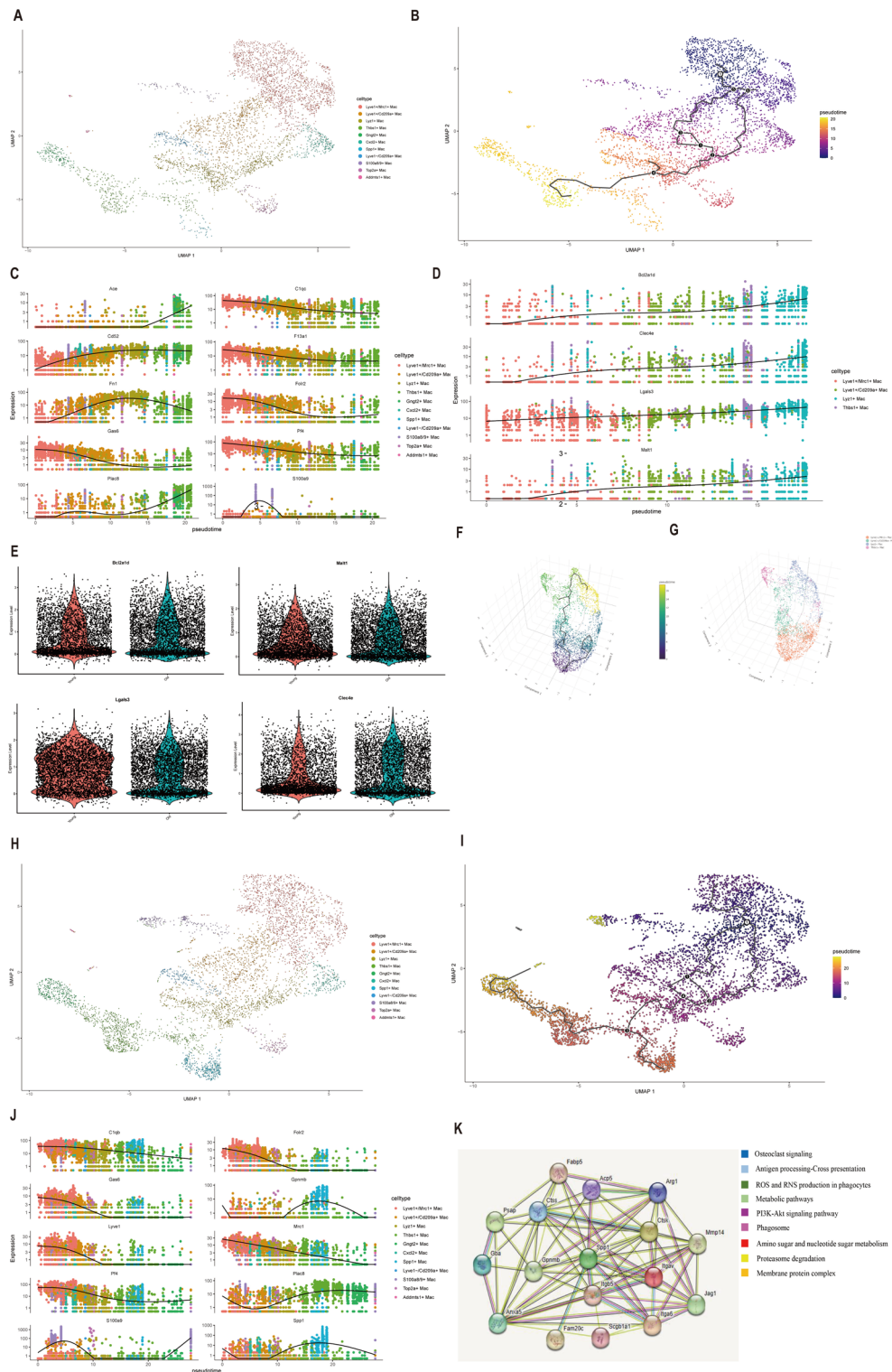
Figure 6. Pseudo-time analysis of SkM macrophages in mice. (**A**) UMAP plot exhibited SkM macrophage subpopulations of Y mice. (**B**) UMAP presenting pseudo-time trajectory of macrophages from Y mice SkM using Monocle 3. (**C**) Changes of canonical genes expressions in Y SkM macrophages along the pseudo-time trajectory. (**D**) Scatter plot showing the expression trend of genes related to the immune response-regulating signaling pathway. (**E**) Violin plot showing the expressions of Bcl2a1d, malt1, Lgals3, Clec4e in SkM macrophages of aging mice. (**F**) 3D Scatterplot representing Lyve1+/Mrc1+ Mac, Lyve1+/Cd209a+ Mac, Lyz1+ Mac, and Thbs1+ Mac. (**G**) 3D Scatterplot showing pseudo-time trajectory in Lyve1+/Mrc1+ Mac, Lyve1+/Cd209a+ Mac, Lyz1+ Mac, and Thbs1+ Mac. (**H**) UMAP illustrates different SkM macrophage subpopulations in O mice with Monocle 3. (**I**) UMAP presents the pseudo-time trajectory of macrophages from aging mice SkM using Monocle 3. (**J**) Changes of canonical genes expressions in O SkM macrophages along the pseudo-time trajectory. (**K**) PPI network of SPP1 co-regulated genes. 3D, three-dimension; Y, young; O, old.

response-regulating signaling pathway took a vital role in keeping the normal polarization of macrophages in young mice SkM. In the meantime, the function and co-regulated association of SPP1 have also been explored.

Spp1 promoted a unique cell–cell communication in aging SkM macrophages

To unveil and compare the intercellular communications networks of different types of macrophages in young and old mice SkM, cell–cell interaction analysis was implemented using CellChat[29]. In the SkM macrophages from Y mice, most signaling patterns, which included CCL, GALECTIN, VISFATIN, etc., were sent from Lyve1+/Cd209a+ Mac. S100a8/9+ Mac received most signaling patterns, including MIF, CXCL, ANNEXIN, etc. (Fig. 7A,B). In aging SkM macrophages, SPP1+ Mac performed a significant role in the majority of outgoing signaling pathways, comprising SPP1, TNF, MIF, etc. Lyve1+/Cd209a+ Mac and S100a8/9+ Mac received most of the signaling. Compared to young SkM macrophages, a unique SPP1-mediated signaling was unveiled (Fig. 7C,D). Ligand receptors regulated by Lyve1+/Cd209a+ Mac were investigated as they sent most signals in SkM of young mice, and ccl2-ccr2 was finally identified (Fig. 7E). Equally, the signaling network activated by SPP1+ Mac was illustrated, and Spp1-Cd44 was present in nearly all SkM macrophage subpopulations (Fig. 7F). SPP1+ Mac played a key part as the sender, mediator, and influencer in the SPP1 signaling pathway network. Lyve1+/Cd209a+ Mac and Gngt2+ Mac mainly acted as receivers (Fig. 7G,H). In addition, Spp1-Cd44 made the greatest contribution to the SPP1 signaling pathway network (Fig. 7I). Almost all aging SkM macrophage subgroups held high levels of Spp1 induced receptors (Fig. 7J). Further, CD44 expression was significantly decreased in skeletal muscle Mac of old mice (Fig. 7K). Lastly, the communication patterns were shown in aging SkM macrophages for comprehending the synergistic effect of signaling pathways among the target cells and the secreting cells. By this means, we discovered a synergy among the SPP1 signal network, CCL, MIF, and other signals in the incoming communication pattern (Fig. 7L). When SPP1+ Mac served as secreting cells, the SPP1 and VEGF signaling were synergetic and mostly dominated by SPP1+ Mac (Fig. 7M). Conclusively, our results displayed that the abundance and peculiarity of SPP1 signaling network communication patterns in aging SkM macrophages compared to macrophages of young mice SkM, and the Spp1-Cd44 receptor-ligands binding pattern contributed mostly to this network.

SPP1+ Mac increased in old mice SkM, and a senotherapeutic drug decreased the proportion of SPP1+ macrophage in vivo models

Despite the fact that we have exhibited through elaborate bioinformatics analysis that SPP1+ Mac was significant during skeletal muscle aging, confirmation through in vivo experiments is indispensable. Of note, previous studies suggested Senolytics have great potential to eliminating senescent cells in multiple diseases[37,38], however, their effect on aging macrophages is unknown. Therefore, the young, old-vehicle, and old-DQ mice SkM models were then constructed to verify the role of SPP1+ Mac (Fig. 8A). We first evaluated body composition and quadriceps weight in three mice groups. Old-Veh mice showed higher body weight and quadriceps weight but lower lean mass when compared to young mice; however, there was no statistical difference in these parameters between old-Veh and old-DQ mice (Fig. 8B–E). Furthermore, we observed an increased proportion of centrally nucleated fibers in old-Veh mice compared with young mice but significantly decreased in old-DQ mice compared to old-Veh mice (Fig. 8F). These results indicated significant senescence-associated phenotypes were exhibited in aging mice SkM and could partially attenuate by D + Q treatment. Finally, we calculated and compared the proportion of SPP1+ Mac in young, old-Veh, and old-DQ mice groups. Confocal IF results revealed that SPP1+ Mac was significantly more abundant in the Old-Veh mice group compared with that in the young mice, while the reduced abundance of SPP1+ Mac in Old-DQ was found when compared to the Old-Veh group (Fig. 8G). In conclusion, the proportion of SPP1+ Mac is elevated in vivo aging mice model, and D + Q contributes to the reduction of SPP1+ Mac, which might suggest that administration of D + Q in mice could rescue SkM aging by the clearance of senescent macrophages.

Discussion

This study comprised a comprehensive analysis and depiction of the distinct cell types, particularly macrophages in young and old mice SkM. ECs and FAPs were the most abundant cell populations, and satellite cell abundance was lower in old SkM. Enrichment analysis indicated lipid metabolism and inflammation-related pathways were commonly up-regulated in aging SkM. Further macrophage classification exhibited that Lyve1⁻/MHCII⁺ macrophages were most abundant in SkM. Moreover, we identified a macrophage subgroup called SPP1+ Mac with high senescent characteristics, strong adipogenesis, and angiogenesis capacity, and owned most metabolic activities, especially in liquid metabolism. Differentiation relationships and intercellular communication between young and aging mice SkM macrophages were also explored. We confirmed that the proportion of SPP1+ Mac was increased in aging SkM by in vivo aged mice model. Of note, D + Q treatment could partially eliminate SPP1+ macrophages in mice SkM. Collectively, we identified strong senescence-associated macrophages and unraveled the potential effect of D + Q treatment on SPP1+ Mac.

Prior research on SkM has largely depended on the development and popularization of scRNA-seq, leaving unsolved queries regarding the function of individual cell subsets in SkM and the exploration of macrophage subpopulations between young and aging and identification of senescent macrophages[13,39,40]. To fill that gap, we first integrated four scRNA-seq datasets containing 34,067 cells from young and old mice SkM. Our data demonstrated that Lyve1⁻/MHCII⁺ Mac was the most abundant macrophage in SkM, accounting for approximately 40% of total macrophages, and was proved to be consistent with previous reports[13,39]. We used another scRNA-seq, which included 9,469 SkM macrophages, to investigate further, and SPP1+ macrophages were elevated in old SkM and identified with remarked ageing features and higher adipogenesis and angiogenesis capacities. Intermuscular adipose tissues were found to increase in aged SkM[5], while angiogenesis in SkM, especially arterioles and
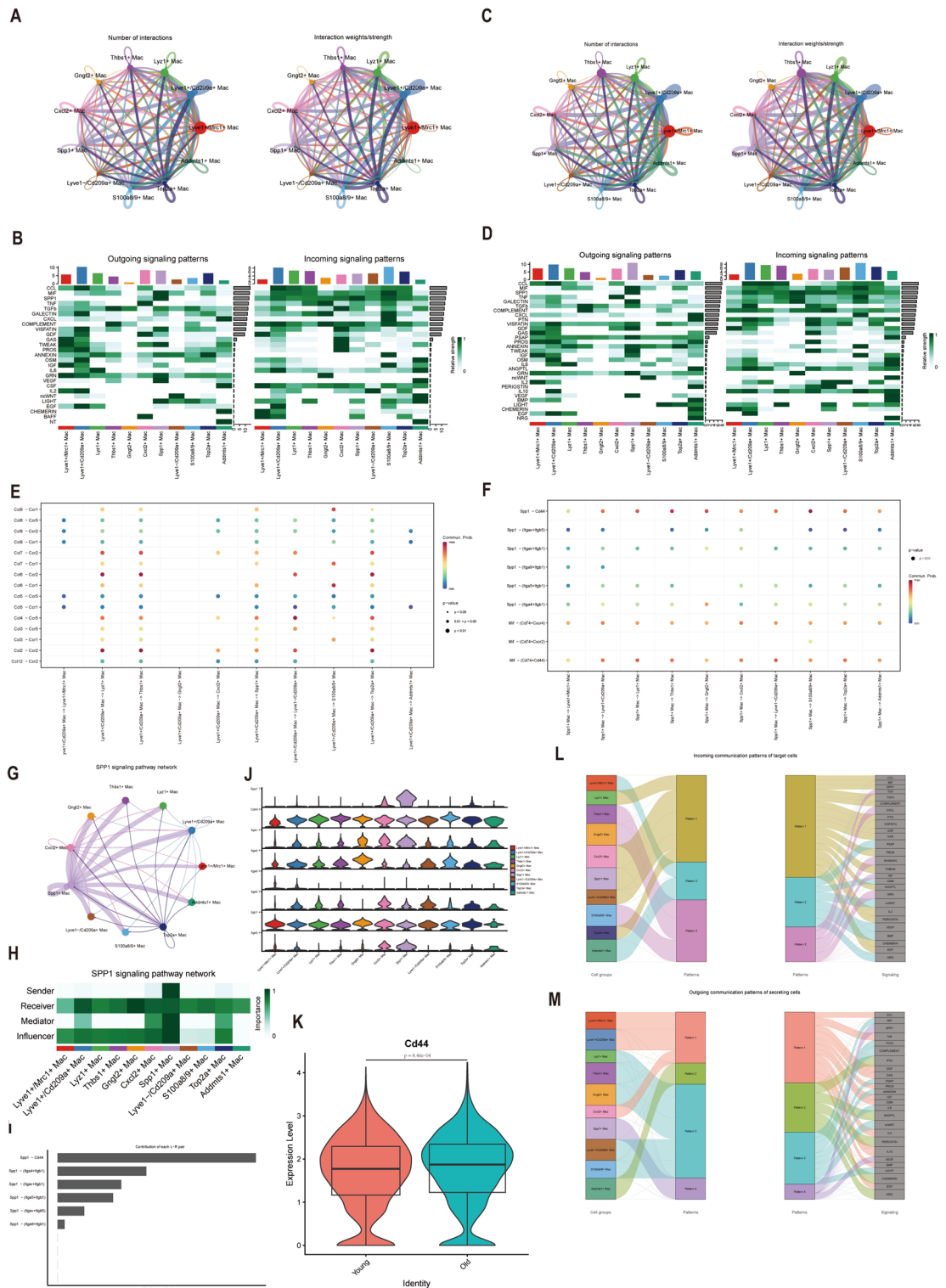
Figure 7. Developmental relationships and communication of SkM macrophages in Y and O mice. (**A**) The quantity and strength of signals for SkM macrophage subgroups in Y mice. (**B**) Comparison of the intensity of enriched outgoing and incoming signals in Mac subgroups from Y mice SkM. (**C**) The quantity and strength of signals for SkM macrophage subgroups in O mice. (**D**) Comparison of the intensity of enriched outgoing and incoming signals in Mac subgroups from O mice SkM. (**E**) L-R interaction contributions in signals emitted by Lyve1+/Cd209a+ Mac. (**F**) L-R interaction contributions in signals emitted by SPP1+ Mac. (**G**) Exhibition of SPP1 signaling pathway between distinct macrophage subgroups of mice SkM using circle plot. (**H**) Investigation of the function of distinct SkM macrophage subgroups in the SPP1 signaling pathway. (**I**) Exhibition of each L-R pair's contribution in SPP1 signaling pathway using the bar plot. (**J**) Illustration of SPP1 signaling pathway-associated genes expressions in SkM macrophage subgroups via the violin plot. (**K**) Comparison of CD44 expression level in SPP1+ macrophages of Y and O mice SkM using a scatterplot. (**L**, **M**) Alluvial plot of targeted cells' incoming and outgoing communication patterns. L-R, ligand-receptor. Y, young. O, old. Mac, macrophages.
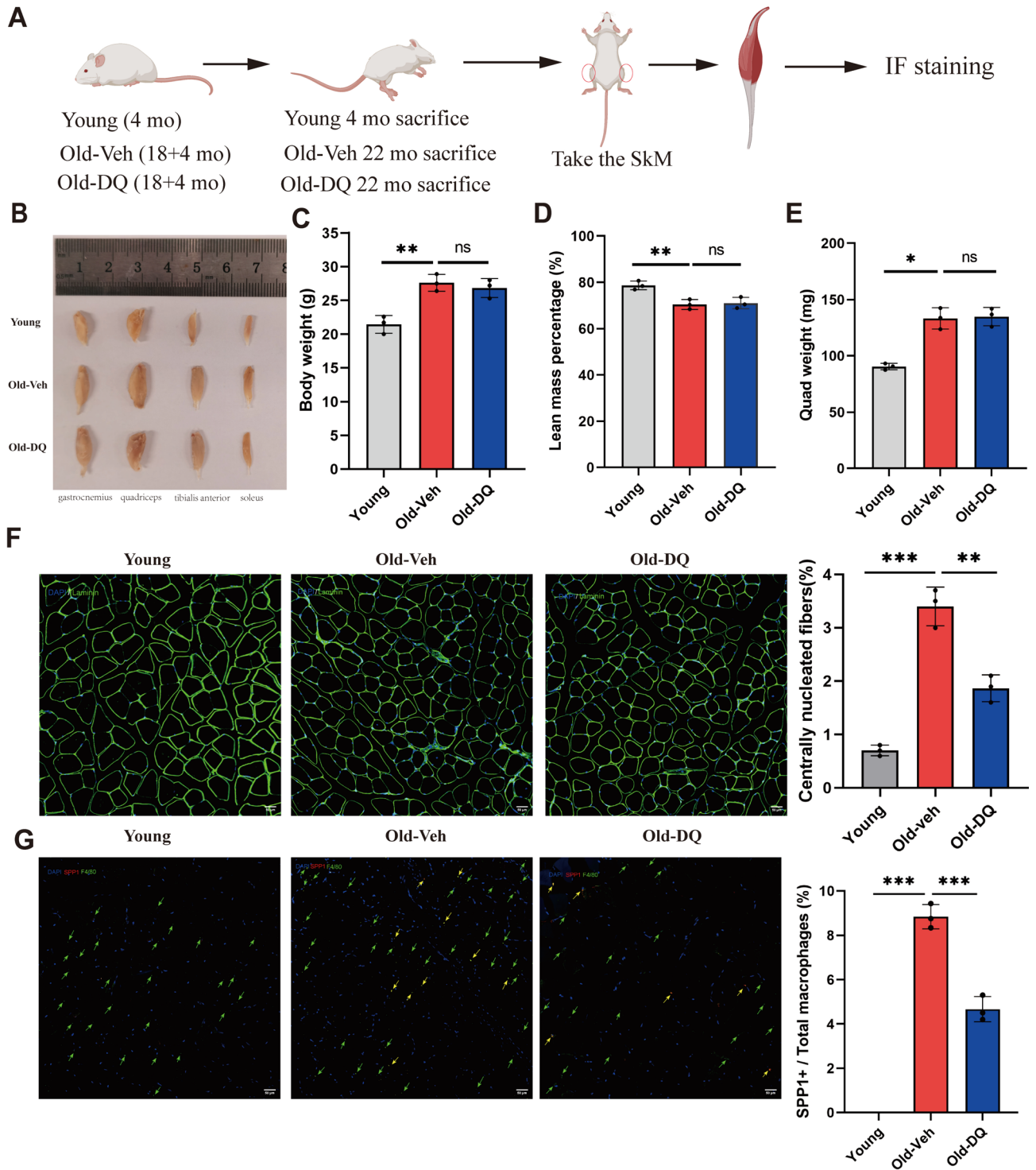
Figure 8. SPP1+ macrophages were increased in SkM of the aging mice model, and senolytics decreased its proportion in vivo. (**A**) The diagram presents the experimental process. (**B**–**E**) Illustration of the gastrocnemius, quadriceps, tibialis anterior, and soleus in young, Old-Veh, and Old-DQ male mice group (**B**). Comparison of body weight (**C**), lean mass percentage (**D**), and quadriceps muscle weight (**E**) between distinct groups (n = 3 per group). (**F**) IF pictures of quadriceps cross-sections stained for Laminin in different groups. (**G**) Confocal microscopy of quadriceps IF staining exhibited F4/80 (green) positive and SPP1 (red) double positive (yellow arrows) SPP1+ macrophages in quadriceps of different groups (n = 3 per group). IF, immunofluorescence. SkM, skeletal muscle. Ns, no significant *, **, *** represent p value less than 0.05, 0.01, 0.001 respectively. Y, young; O, old.

capillaries, was demonstrated to play significant roles in meeting properties exchange and metabolic demands[35,41]. Our results suggested SPP1+ macrophages in SkM might be involved in adipogenesis and capillary angiogenesis during SkM aging.

Metabolism in SkM proves critical for the hold of both mechanical and metabolic activities of SkM. Thus, an in-depth analysis of SkM metabolism throughout the aging process can be beneficial in alleviating senescent SkM function. It has been proved that physical exercises and decreased energy intake can improve aging SkM metabolism, mainly via facilitating fatty acid oxidation and increasing antioxidative capacity[42]. Macrophages play a crucial role in regulating activities that attempt to maintain homeostasis and significantly influence both inflammatory and immune responses, but they also assist in keeping metabolic stability[43]. Moreover, macrophages exhibit a high degree of versatility, which means they react to environmental signals and appropriately transform their phenotypes and functions[44,45]. In this study, we analyzed and compared the metabolism of all cell types in SkM, as well as 11 distinct SkM macrophage populations. Lipid metabolism, like Glycerophospholipid metabolism, and carbohydrate metabolism, such as Glycolysis/Gluconeogenesis and Pentose phosphate pathway, were up-regulated in macrophages of aging SkM. Importantly, enrichment analysis suggested differences between macrophage clusters and SPP1+ macrophages were the most active in lipid metabolism like Glycerolipid metabolism, Glycosphingolipid metabolism, and Sphingolipid metabolism. These results agree with the previous study, which we explored in more detail.

Osteopontin (SPP1) has been recognized as an ingredient of the inflammatory circumstances in mdx muscles, and also been demonstrated to connect with infiltrating macrophages in mouse muscle regeneration[46,47]. Previous study has raised the vital function of macrophage-derived osteopontin in the inflammatory stage during muscle regeneration[48]. In this study, we recognized a macrophages subgroup featured by high SPP1 expression and own appreciably senescent score during skeletal aging. With the development of single-cell sequencing, SPP1+ macrophages have been reported to be involved in the progression of multiple diseases, like dystrophic muscle[49], colorectal cancer[50,51], idiopathic pulmonary fibrosis[52], heart failure[53,54], and human chronic kidney disease[54]. In general, SPP1+ macrophages mainly accumulate in the pathological tissues and are usually associated with poor prognosis[50,55]. Notably, Zhang et al.[56] suggested aging FAPs recruited macrophages via SPP1/CCL2 and promoted polarization toward an M2 subtype. Importantly, FAPs are reported to be the main source of colony-stimulating factor 1(CSF1) in skeletal muscle and play a vital role in self-renewing tissue-resident macrophages[57]. Our study discovered that SPP1+ macrophages were increased significantly in the old quadriceps compared with the quadriceps of young mice. Meanwhile, this subcluster of macrophages also highly expressed Gpnmb, recognized as a transmembrane marker of senescence[58]. Of note, SPP1+ macrophages in SkM with high expression of Fabp5, which are related to long-chain fatty acid transporters, binding to SPP1+ macrophages own a higher adipogenesis score; we inferred that this subcluster of macrophages might play an important role in the formation of intermuscular adipose tissues of aging mice. However, the exact mechanisms behind these warrant further studies.

The Senolytic cocktail of D + Q has been extensively explored in SkM aging to improve SkM molecular profile and function[23,59]. Previous studies have shown that D + Q treatment affects cells in muscle, for example, increased myogenic progenitor cell proliferation in vitro[60]. Of note, D + Q could markedly reduce the number of centrally nucleated fibers but could not attenuate age-related reductions in SkM mass and myofiber cross-sectional area[16]. In this study, we observed that DQ treatment had no significant effect on body weight, lean mass, or quadriceps weights. Further, a significant reduction in the percentage of centrally nucleated fibers in the DQ group suggested that DQ administration partially improved aged-related phenotypes of SkM. Importantly, we first validated that SPP1+ macrophages are mainly distributed in aging SkM, and DQ somewhat reduced its proportion in vivo.

Limitation

The current research is exposed to several limitations. Although we identified a unique macrophages subgroup highly expressed SPP1 and play an important role during SkM aging, more experiments should be implemented to unveil the underlying mechanisms by which SPP1+ macrophages involved in the formation of intermuscular adipose tissue and angiogenesis. Meanwhile, SPP1+ macrophages increased during mouse SkM aging; however, this result still needs to be validated in human specimens.

Conclusion

Our present work concluded that a macrophage subgroup mainly distributed in aging mice SkM with high SPP1 expression was recognized. Subsequent research revealed that SPP1+ Mac exhibited more senescent feature and adipogenesis capacity. Distinct correlations in young and old SkM macrophages were illustrated. In addition, distinctions in metabolic pathways and cell–cell communication were analyzed. Finally, we validated that SPP1+ macrophages were significantly increased in the old SkM, and D + Q treatment could alleviate their proportion in vivo. However, further research is required to explore the biological effect of SPP1+ macrophages in aging mice SkM and its relationships with intermuscular adipogenesis. Overall, our study offers fresh insights into understanding the SkM macrophage differentiation process in young mice and the significance of SPP1+ macrophages in the progression of SkM aging.

Data availability

References

1. Chen, X. *et al.* The path to healthy ageing in China: A Peking University-lancet commission. *Lancet (London, England)* **400**(10367), 1967–2006 (2022).
2. Hayes, N., Fogarty, M., Sadofsky, L. & Jones, H. S. Physiologically-obtainable polyphenol exposures modulate reactive oxygen and nitrogen species signaling in the C2C12 model of skeletal muscle ageing. *Eur. J. Pharmacol.* **941**, 175511 (2023).
3. Jung, H. J., Lee, K. P., Kwon, K. S. & Suh, Y. MicroRNAs in skeletal muscle aging: Current issues and perspectives. *J. Gerontol. A Biol. Sci. Med. Sci.* **74**(7), 1008–1014 (2019).
4. Fukada, K. & Kajiya, K. Age-related structural alterations of skeletal muscles and associated capillaries. *Angiogenesis* **23**(2), 79–82 (2020).
5. Cui, C. Y. *et al.* Skewed macrophage polarization in aging skeletal muscle. *Aging Cell* **18**(6), e13032 (2019).
6. Tidball, J. G. Regulation of muscle growth and regeneration by the immune system. *Nat. Rev. Immunol.* **17**(3), 165–178 (2017).
7. Scala, P. *et al.* Stem cell and macrophage roles in skeletal muscle regenerative medicine. *Int. J. Mol. Sci.* **22**(19), 10867 (2021).
8. Zhang, J. *et al.* Endothelial lactate controls muscle regeneration from ischemia by inducing M2-like macrophage polarization. *Cell Metab.* **31**(6), 1136-1153.e1137 (2020).
9. Chen, Y. F., Lee, C. W., Wu, H. H., Lin, W. T. & Lee, O. K. Immunometabolism of macrophages regulates skeletal muscle regeneration. *Front. Cell Dev. Biology* **10**, 948819 (2022).
10. Sorensen, J. R. *et al.* An altered response in macrophage phenotype following damage in aged human skeletal muscle: Implications for skeletal muscle repair. *FASEB J. Off. Publ. Fed. Am. Soc. Exp. Biol.* **33**(9), 10353–10368 (2019).
11. Ahmadi, M. *et al.* Aging is associated with an altered macrophage response during human skeletal muscle regeneration. *Exp. Gerontol.* **169**, 111974 (2022).
12. Wang, Y., Wehling-Henricks, M., Samengo, G. & Tidball, J. G. Increases of M2a macrophages and fibrosis in aging muscle are influenced by bone marrow aging and negatively regulated by muscle-derived nitric oxide. *Aging Cell* **14**(4), 678–688 (2015).
13. Krasniewski, L. K. *et al.* Single-cell analysis of skeletal muscle macrophages reveals age-associated functional subpopulations. *eLife* **11**, e77974 (2022).
14. Stuart, T. *et al.* Comprehensive integration of single-cell data. *Cell* **177**(7), 1888-1902.e1821 (2019).
15. Korsunsky, I. *et al.* Fast, sensitive and accurate integration of single-cell data with Harmony. *Nat. Methods* **16**(12), 1289–1296 (2019).
16. Zhang, X. *et al.* Characterization of cellular senescence in aging skeletal muscle. *Nat. Aging* **2**(7), 601–615 (2022).
17. De Micheli, A. J. *et al.* Single-cell analysis of the muscle stem cell hierarchy identifies heterotypic communication signals involved in skeletal muscle regeneration. *Cell Rep.* **30**(10), 3583-3595.e3585 (2020).
18. McKellar, D. W. *et al.* Large-scale integration of single-cell transcriptomic data captures transitional progenitor states in mouse skeletal muscle regeneration. *Commun. Biol.* **4**(1), 1280 (2021).
19. Walter, L. D., Orton, J. L., Hannah Fong, E. H., Maymi, V. I., Rudd, B. D., Elisseeff, J. H., Cosgrove, B. D. Single-cell transcriptomic analysis of skeletal muscle regeneration across mouse lifespan identifies altered stem cell states associated with senescence. *bioRxiv* (2023).
20. Butler, A., Hoffman, P., Smibert, P., Papalexi, E. & Satija, R. Integrating single-cell transcriptomic data across different conditions, technologies, and species. *Nat. Biotechnol.* **36**(5), 411–420 (2018).
21. Franzén, O., Gan, L. M. & Björkegren, J. L. M. PanglaoDB: A web server for exploration of mouse and human single-cell RNA sequencing data. *Datab. J. Biol. Datab. Curation* **2019**, baz046 (2019).
22. Zhou, Y. *et al.* Metascape provides a biologist-oriented resource for the analysis of systems-level datasets. *Nat. Commun.* **10**(1), 1523 (2019).
23. Saul, D. *et al.* A new gene set identifies senescent cells and predicts senescence-associated pathways across tissues. *Nat. Commun.* **13**(1), 4827 (2022).
24. Qu, Y. *et al.* A comprehensive analysis of single-cell RNA transcriptome reveals unique SPP1+ chondrocytes in human osteoarthritis. *Comput. Biol. Med.* **160**, 106926 (2023).
25. Browaeys, R., Saelens, W. & Saeys, Y. NicheNet: Modeling intercellular communication by linking ligands to target genes. *Nat. Methods* **17**(2), 159–162 (2020).
26. Wu, Y. *et al.* Spatiotemporal immune landscape of colorectal cancer liver metastasis at single-cell level. *Cancer Discov.* **12**(1), 134–153 (2022).
27. Qiu, X. *et al.* Reversed graph embedding resolves complex single-cell trajectories. *Nat. Methods* **14**(10), 979–982 (2017).
28. Cao, J. *et al.* The single-cell transcriptional landscape of mammalian organogenesis. *Nature* **566**(7745), 496–502 (2019).
29. Jin, S. *et al.* Inference and analysis of cell-cell communication using Cell Chat. *Nat. Commun.* **12**(1), 1088 (2021).
30. Szklarczyk, D. *et al.* The STRING database in 2021: Customizable protein-protein networks, and functional characterization of user-uploaded gene/measurement sets. *Nucleic Acids Res.* **49**(D1), D605-d612 (2021).
31. Kowalczyk, M. S. *et al.* Single-cell RNA-seq reveals changes in cell cycle and differentiation programs upon aging of hematopoietic stem cells. *Genome Res.* **25**(12), 1860–1872 (2015).
32. Akasaki, Y. *et al.* Glycolytic fast-twitch muscle fiber restoration counters adverse age-related changes in body composition and metabolism. *Aging Cell* **13**(1), 80–91 (2014).
33. Lin, J. *et al.* Senolytics prevent caveolar Ca(V) 3.2-RyR axis malfunction in old vascular smooth muscle. *Aging cell* **22**(11), e14002 (2023).
34. Giordani, L. *et al.* High-dimensional single-cell cartography reveals novel skeletal muscle-resident cell populations. *Mol. Cell* **74**(3), 609-621.e606 (2019).
35. Li, P. *et al.* Microbiota derived D-malate inhibits skeletal muscle growth and angiogenesis during aging via acetylation of Cyclin A. *EMBO Rep.* **25**(2), 524–543 (2024).
36. Chazaud, B. Inflammation and skeletal muscle regeneration: Leave it to the macrophages!. *Trends Immunol.* **41**(6), 481–492 (2020).
37. Hickson, L. J. *et al.* Senolytics decrease senescent cells in humans: Preliminary report from a clinical trial of Dasatinib plus Quercetin in individuals with diabetic kidney disease. *EBioMedicine* **47**, 446–456 (2019).
38. Chaib, S., Tchkonia, T. & Kirkland, J. L. Cellular senescence and senolytics: The path to the clinic. *Nat. Med.* **28**(8), 1556–1568 (2022).
39. Cui, C. Y., Ferrucci, L. & Gorospe, M. Macrophage involvement in aging-associated skeletal muscle regeneration. *Cells* **12**(9), 1214 (2023).
40. Wang, X. *et al.* Heterogeneous origins and functions of mouse skeletal muscle-resident macrophages. *Proc. Natl. Acad. Sci. U. S. A.* **117**(34), 20729–20740 (2020).
41. Parise, G. *et al.* Capillary facilitation of skeletal muscle function in health and disease. *Appl. Physiol. Nutr. Metab. Physiol. Appl. Nutr. Metab.* **45**(5), 453–462 (2020).
42. Thonusin, C. *et al.* Exercise and caloric restriction exert different benefits on skeletal muscle metabolism in aging condition. *Nutrients* **15**(23), 5004 (2023).

43. van Beek, A. A., Van den Bossche, J., Mastroberardino, P. G., de Winther, M. P. J. & Leenen, P. J. M. Metabolic alterations in aging macrophages: Ingredients for inflammaging?. *Trends Immunol.* **40**(2), 113–127 (2019).
44. Locati, M., Curtale, G. & Mantovani, A. Diversity, mechanisms, and significance of macrophage plasticity. *Ann. Rev. Pathol.* **15**, 123–147 (2020).
45. Wynn, T. A., Chawla, A. & Pollard, J. W. Macrophage biology in development, homeostasis and disease. *Nature* **496**(7446), 445–455 (2013).
46. Porter, J. D. *et al.* A chronic inflammatory response dominates the skeletal muscle molecular signature in dystrophin-deficient mdx mice. *Hum. Mol. Genet.* **11**(3), 263–272 (2002).
47. Uaesoontrachoon, K. *et al.* Osteopontin and skeletal muscle myoblasts: Association with muscle regeneration and regulation of myoblast function in vitro. *Int. J. Biochem. Cell Biol.* **40**(10), 2303–2314 (2008).
48. Hirata, A. *et al.* Expression profiling of cytokines and related genes in regenerating skeletal muscle after cardiotoxin injection: A role for osteopontin. *Am. J. Pathol.* **163**(1), 203–215 (2003).
49. Coulis, G. *et al.* Single-cell and spatial transcriptomics identify a macrophage population associated with skeletal muscle fibrosis. *Sci. Adv.* **9**(27), eadd9984 (2023).
50. Qi, J. *et al.* Single-cell and spatial analysis reveal interaction of FAP(+) fibroblasts and SPP1(+) macrophages in colorectal cancer. *Nat. Commun.* **13**(1), 1742 (2022).
51. Sathe, A. *et al.* Colorectal cancer metastases in the liver establish immunosuppressive spatial networking between tumor-associated SPP1+ macrophages and fibroblasts. *Clin. Cancer Res. Off. J. Am. Assoc. Cancer Res.* **29**(1), 244–260 (2023).
52. Morse, C. *et al.* Proliferating SPP1/MERTK-expressing macrophages in idiopathic pulmonary fibrosis. *Eur. Respir. J.* **54**(2), 1802441 (2019).
53. Fu, M. *et al.* Single-cell RNA sequencing of coronary perivascular adipose tissue from end-stage heart failure patients identifies SPP1(+) macrophage subpopulation as a target for alleviating fibrosis. *Arterioscler. Thromb. Vasc. Biol.* **43**(11), 2143–2164 (2023).
54. Hoeft, K. *et al.* Platelet-instructed SPP1(+) macrophages drive myofibroblast activation in fibrosis in a CXCL4-dependent manner. *Cell Rep.* **42**(2), 112131 (2023).
55. Yu, S., Chen, M., Xu, L., Mao, E. & Sun, S. A senescence-based prognostic gene signature for colorectal cancer and identification of the role of SPP1-positive macrophages in tumor senescence. *Front. Immunol.* **14**, 1175490 (2023).
56. Zhang, X. *et al.* Senescent skeletal muscle fibroadipogenic progenitors recruit and promote M2 polarization of macrophages. *Aging Cell* **23**(3), e14069 (2024).
57. Babaeijandaghi, F. *et al.* DPPIV(+) fibro-adipogenic progenitors form the niche of adult skeletal muscle self-renewing resident macrophages. *Nat. Commun.* **14**(1), 8273 (2023).
58. Suda, M. *et al.* Senolytic vaccination improves normal and pathological age-related phenotypes and increases lifespan in progeroid mice. *Nat. Aging* **1**(12), 1117–1126 (2021).
59. Xu, M. *et al.* Senolytics improve physical function and increase lifespan in old age. *Nat. Med.* **24**(8), 1246–1256 (2018).
60. Dungan, C. M. *et al.* Deletion of SA β-Gal+ cells using senolytics improves muscle regeneration in old mice. *Aging Cell* **21**(1), e13528 (2022).

Author contributions

Conception, bioinformatics analysis, experiment, and manuscript draft were done by W.B.; acquisition of data (acquired and managed patients, provided facilities, etc.), and sample collection was performed by M.Y., M.S., and M.H.; C.J., W.G. and G.F. contributed funding acquisition and supervision. All authors read the final version of this manuscript and endorsed for publication.

Funding

Competing interests

The authors declare no competing interests.

Additional information

Supplementary Information The online version contains supplementary material available at https://doi.org/10.1038/s41598-024-69284-9.

Correspondence and requests for materials should be addressed to G.F. or W.G.

Reprints and permissions information is available at www.nature.com/reprints.

Publisher's note Springer Nature remains neutral with regard to jurisdictional claims in published maps and institutional affiliations.